

# Synthesis, Structure and Oxygen-evolving Activity of Dinuclear Manganese Complexes with a Schiff-base Macrocyclic Ligand and Bridging Benzoate†

Toshi Nagata and Junji Mizukami

Department of Chemistry, Kyoto University, Kyoto 606-01, Japan

A series of dinuclear manganese complexes  $[\text{Mn}_2\text{L}(\text{RCO}_2)]\text{ClO}_4$ , where  $\text{RCO}_2\text{H}$  is a substituted benzoic acid and  $\text{H}_2\text{L}$  is a Schiff-base macrocyclic ligand formed by a 2:2 condensation of 2,6-diformyl-4-methylphenol and *N,N*-bis(2-aminoethyl)methylamine, were synthesized. The crystal structure ( $\text{R} = 2\text{-O}_2\text{NC}_6\text{H}_4$ ) showed the presence of two crystallographically independent complex cations with slightly different conformations. The difference can be attributed to the crystal packing effect. These complexes catalysed disproportionation of  $\text{H}_2\text{O}_2$ ; the activities showed a characteristic V-shaped dependence with  $\text{p}K_a$  of  $\text{RCO}_2\text{H}$ , which suggests the importance of protonation prior to dissociation of  $\text{RCO}_2^-$ .

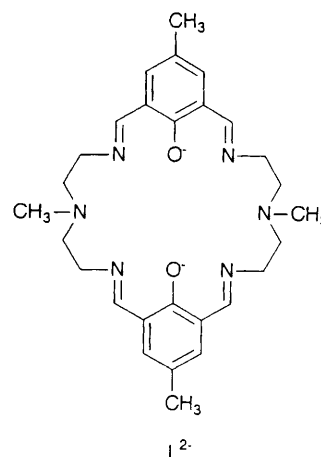
Recently much attention has been focused on manganese clusters related to oxygen evolution in biological systems, among which manganese catalase<sup>1</sup> and the oxygen evolving complex of plant photosynthesis<sup>2</sup> are of major interest. However, the mechanism of oxygen evolution in these systems is still far from completely understood. There have been several reports on manganese complexes as simplified model compounds for oxygen evolution,<sup>3-10</sup> which have proven to be useful, both for accumulating knowledge on oxygen evolution from a chemical point of view and for an initial step to mimic photosynthesis in artificial systems.

We previously reported<sup>11</sup> the synthesis and structure of, and oxygen evolution by, a series of dimanganese complexes of the Schiff-base macrocyclic ligand  $\text{H}_2\text{L}$  the [2 + 2] condensation product of 2,6-diformyl-4-methylphenol and *N,N*-bis(2-aminoethyl)methylamine. This ligand shares the advantages (ease of preparation; stability of its complexes due to entropy effects; the phenolic oxygens serving as binders of two manganese ions) with other Schiff-base ligands that have been used for studies with manganese.<sup>9,10,12</sup> Moreover, our ligand has a unique advantage that it can co-ordinate to ten out of twelve ligating sites of two octahedral manganese ions in a binuclear complex, so leaving only two vacant positions for external ligand(s). This particular structural property makes our complexes especially suitable for studies on catalytic reactions.

In this article, we report the synthesis of a series of complexes  $[\text{Mn}_2\text{L}(\text{RCO}_2)]\text{ClO}_4$ , where  $\text{RCO}_2^-$  is a substituted benzoate anion. The crystal structure ( $\text{R} = 2\text{-O}_2\text{NC}_6\text{H}_4$ ) and electrochemical behaviour are very similar to those of previously reported acetate complexes ( $\text{R}' = \text{CH}_3\text{X}_{3-n}$ ,  $\text{X} = \text{F}$  or  $\text{Cl}$ ).<sup>11</sup> These complexes also catalysed the disproportionation reaction of hydrogen peroxide, and the catalytic activities change in a characteristic manner with the basicity of the bridging carboxylate, showing a minimum at  $\text{p}K_a(\text{RCO}_2\text{H}) \approx 2$ . We present a rational explanation by considering protonation of the complex prior to dissociation of the bridging carboxylate.

## Results and Discussion

**Synthesis and Structure.**—A series of complexes  $[\text{Mn}_2\text{L}(\text{RCO}_2)]\text{ClO}_4$  ( $\text{R} = \text{Ph}$ ,  $\text{XC}_6\text{H}_4$  ( $\text{X} = 4\text{-MeO}$ ,  $4\text{-Me}$ ,  $4\text{-Br}$ ,  $4\text{-Cl}$ ,  $4\text{-F}$ ,  $4\text{-NO}_2$ ,  $2\text{-MeO}$ ,  $2\text{-Me}$ ,  $2\text{-Br}$ ,  $2\text{-Cl}$ ,  $2\text{-F}$  or  $2\text{-NO}_2$ ),  $\text{XYC}_6\text{H}_3$  [ $\text{XY} = 2,4\text{-(NO}_2)_2$ ,  $3,4\text{-(NO}_2)_2$  or  $2\text{-Cl-4-NO}_2$ ]) were synthesized by template condensation of *N,N*-bis(2-aminoethyl)methylamine, 2,6-diformyl-4-methylphenol,  $\text{RCO}_2\text{Na}$  and  $\text{Mn}(\text{ClO}_4)_2 \cdot 6\text{H}_2\text{O}$ . The crystal structure was investigated for  $[\text{Mn}_2\text{L}(2\text{-O}_2\text{NC}_6\text{H}_4\text{CO}_2)]\text{ClO}_4$  and fractional coordinates are compiled in Table 1. Bond lengths and angles around the manganese ions of both molecules are listed in Table 2. The asymmetric unit of the triclinic unit cell contains two crystallographically independent complex cations  $[\text{Mn}_2\text{L}(2\text{-O}_2\text{NC}_6\text{H}_4\text{CO}_2)]^+$ , two perchlorate anions and one  $\text{Me}_2\text{NCHO}$  solvate molecule. One of the two independent complex cations (molecule A) is shown in Fig. 1; the other one (molecule B) has a similar configuration, but with a significant difference in the angle between the two vectors  $\text{O}(1)\text{-C}(1)$  and  $\text{O}(2)\text{-C}(15)$ ;  $141.7(8)$  and  $123.7(9)^\circ$  for molecules A and B, respectively. The larger angle in molecule A can be attributed to packing forces in the crystal. Fig. 2 shows part of the crystal, containing molecules A and B, and their symmetry-related partners A' and B' (symmetry operation:  $-x, -y, 1-z$ ) with dashed lines showing short contacts ( $< 3.60 \text{ \AA}$ ). The atoms and distances involved in these short contacts are listed in Table 3. Molecule A has ten contacts with molecule B', of which eight are related with the carbon atoms of the two phenol rings. These contacts



Br, 4-Cl, 4-F, 4-NO<sub>2</sub>, 2-MeO, 2-Me, 2-Br, 2-Cl, 2-F or 2-NO<sub>2</sub>),  $\text{XYC}_6\text{H}_3$  [ $\text{XY} = 2,4\text{-(NO}_2)_2$ ,  $3,4\text{-(NO}_2)_2$  or  $2\text{-Cl-4-NO}_2$ ]) were synthesized by template condensation of *N,N*-bis(2-aminoethyl)methylamine, 2,6-diformyl-4-methylphenol,  $\text{RCO}_2\text{Na}$  and  $\text{Mn}(\text{ClO}_4)_2 \cdot 6\text{H}_2\text{O}$ . The crystal structure was investigated for  $[\text{Mn}_2\text{L}(2\text{-O}_2\text{NC}_6\text{H}_4\text{CO}_2)]\text{ClO}_4$  and fractional coordinates are compiled in Table 1. Bond lengths and angles around the manganese ions of both molecules are listed in Table 2. The asymmetric unit of the triclinic unit cell contains two crystallographically independent complex cations  $[\text{Mn}_2\text{L}(2\text{-O}_2\text{NC}_6\text{H}_4\text{CO}_2)]^+$ , two perchlorate anions and one  $\text{Me}_2\text{NCHO}$  solvate molecule. One of the two independent complex cations (molecule A) is shown in Fig. 1; the other one (molecule B) has a similar configuration, but with a significant difference in the angle between the two vectors  $\text{O}(1)\text{-C}(1)$  and  $\text{O}(2)\text{-C}(15)$ ;  $141.7(8)$  and  $123.7(9)^\circ$  for molecules A and B, respectively. The larger angle in molecule A can be attributed to packing forces in the crystal. Fig. 2 shows part of the crystal, containing molecules A and B, and their symmetry-related partners A' and B' (symmetry operation:  $-x, -y, 1-z$ ) with dashed lines showing short contacts ( $< 3.60 \text{ \AA}$ ). The atoms and distances involved in these short contacts are listed in Table 3. Molecule A has ten contacts with molecule B', of which eight are related with the carbon atoms of the two phenol rings. These contacts

† Supplementary data available: see Instructions for Authors, *J. Chem. Soc., Dalton Trans.*, 1995, Issue 1, pp. xxv-xxx.

**Table 1** Positional parameters for  $[\text{Mn}_2\text{L}(2\text{-O}_2\text{NC}_6\text{H}_4\text{CO}_2)]\text{ClO}_4 \cdot 0.5\text{Me}_2\text{NCHO}$  with estimated standard deviations in parentheses

Atom*	x	y	z	Atom	x	y	z
Mn(1a)	0.4257(1)	0.3693(1)	0.6210(1)	C(17a)	0.4412(8)	0.2058(7)	0.8250(7)
Mn(2a)	0.3490(1)	0.4387(1)	0.7680(1)	C(18a)	0.3810(9)	0.1712(8)	0.8651(8)
Mn(1b)	0.1389(1)	-0.1080(1)	0.2783(1)	C(19a)	0.3190(8)	0.1942(7)	0.8580(8)
Mn(2b)	0.1414(1)	-0.1787(1)	0.4484(1)	C(20a)	0.3168(7)	0.2512(7)	0.8131(7)
Cl(1p)	0.9370(3)	0.1110(3)	0.1869(3)	C(21a)	0.383(1)	0.1135(8)	0.9191(9)
Cl(2p)	0.5391(3)	0.1702(3)	0.2322(3)	C(22a)	0.2557(7)	0.2766(7)	0.8208(8)
O(1a)	0.3253(5)	0.4038(4)	0.6165(5)	C(23a)	0.1909(8)	0.3610(8)	0.8244(8)
O(2a)	0.3803(4)	0.3386(4)	0.7309(5)	C(24a)	0.2544(9)	0.4489(10)	0.9188(9)
O(3a)	0.5314(5)	0.5087(5)	0.7033(5)	C(25a)	0.4211(8)	0.5392(10)	1.0091(8)
O(4a)	0.4915(5)	0.5416(5)	0.8262(5)	C(26a)	0.344(2)	0.588(1)	0.910(1)
O(5a)	0.6894(7)	0.5475(7)	0.8584(7)	C(27a)	0.329(1)	0.599(1)	0.833(1)
O(6a)	0.7955(8)	0.6162(8)	0.815(1)	C(28a)	0.2776(9)	0.5326(8)	0.661(1)
O(1b)	0.0573(4)	-0.1463(4)	0.3625(5)	C(29a)	0.5446(7)	0.5611(7)	0.7850(8)
O(2b)	0.2402(4)	-0.0711(4)	0.4195(4)	C(30a)	0.6298(7)	0.6562(7)	0.8317(7)
O(3b)	0.1101(5)	-0.2370(5)	0.2101(5)	C(31a)	0.7177(8)	0.6793(7)	0.8517(7)
O(4b)	0.1254(5)	-0.2802(4)	0.3319(5)	C(32a)	0.7939(8)	0.7646(9)	0.8866(9)
O(5b)	-0.0582(8)	-0.5418(7)	0.2132(10)	C(33a)	0.7811(9)	0.8326(8)	0.9065(9)
O(6b)	-0.0613(6)	-0.4350(6)	0.1948(7)	C(34a)	0.694(1)	0.8139(8)	0.8886(10)
O(1s)	0.6412(8)	0.2037(9)	0.8923(9)	C(35a)	0.6197(8)	0.7266(8)	0.8516(9)
O(1p)	0.8971(9)	0.160(1)	0.1799(9)	C(1b)	-0.0026(6)	-0.1330(6)	0.3796(7)
O(2p)	1.0100(7)	0.1404(8)	0.1581(7)	C(2b)	-0.0550(7)	-0.1761(7)	0.4280(8)
O(3p)	0.8741(10)	0.0226(9)	0.1275(10)	C(3b)	-0.1187(7)	-0.1591(8)	0.4462(8)
O(4p)	0.9729(8)	0.1275(7)	0.2865(7)	C(4b)	-0.1378(7)	-0.1027(7)	0.4185(8)
O(5p)	0.597(1)	0.206(1)	0.195(1)	C(5b)	-0.0870(8)	-0.0624(7)	0.3701(8)
O(6p)	0.5437(7)	0.1012(8)	0.246(1)	C(6b)	-0.0237(7)	-0.0765(7)	0.3480(7)
O(7p)	0.4510(9)	0.1364(10)	0.180(1)	C(7b)	-0.2077(8)	-0.0882(8)	0.4405(8)
O(8p)	0.570(1)	0.235(1)	0.320(1)	C(8b)	0.0171(8)	-0.0334(7)	0.2920(8)
N(1a)	0.3200(7)	0.2776(6)	0.4687(7)	C(9b)	0.0967(8)	0.0026(7)	0.1933(9)
N(2a)	0.5047(8)	0.3563(7)	0.5077(9)	C(10b)	0.0541(8)	-0.0739(7)	0.0952(8)
N(3a)	0.5190(6)	0.3340(6)	0.6854(7)	C(11b)	0.0026(10)	-0.2315(8)	0.0330(9)
N(4a)	0.2500(5)	0.3355(6)	0.7978(6)	C(12b)	0.163(1)	-0.117(1)	0.0829(10)
N(5a)	0.3417(7)	0.5111(6)	0.9175(6)	C(13b)	0.249(1)	-0.042(1)	0.155(1)
N(6a)	0.3122(7)	0.5317(6)	0.7433(8)	C(14b)	0.3500(8)	0.0093(8)	0.3171(9)
N(7a)	0.7363(7)	0.6093(8)	0.8416(8)	C(15b)	0.3300(7)	-0.0114(6)	0.4669(8)
N(1b)	0.0779(6)	-0.0335(5)	0.2647(6)	C(16b)	0.3868(7)	0.0292(7)	0.4218(8)
N(2b)	0.0826(7)	-0.1354(6)	0.1028(6)	C(17b)	0.4835(8)	0.0890(7)	0.4747(9)
N(3b)	0.2663(6)	-0.0336(6)	0.2568(6)	C(18b)	0.5311(8)	0.1145(7)	0.5754(9)
N(4b)	0.2462(6)	-0.0848(6)	0.5988(6)	C(19b)	0.4756(7)	0.0763(7)	0.6184(8)
N(5b)	0.1662(8)	-0.2647(8)	0.5413(8)	C(20b)	0.3798(7)	0.0162(7)	0.5723(8)
N(6b)	0.0134(7)	-0.2563(7)	0.4623(8)	C(21b)	0.6354(7)	0.1769(7)	0.6287(9)
N(7b)	-0.0291(7)	-0.4790(7)	0.1913(7)	C(22b)	0.3321(8)	-0.0216(8)	0.6272(8)
N(1s)	0.6762(9)	0.1574(8)	1.0081(9)	C(23b)	0.2192(8)	-0.1173(9)	0.6707(8)
C(1a)	0.2722(7)	0.4062(7)	0.5448(8)	C(24b)	0.2133(10)	-0.205(1)	0.647(1)
C(2a)	0.2490(8)	0.4692(8)	0.5639(9)	C(25b)	0.222(1)	-0.298(1)	0.513(1)
C(3a)	0.194(1)	0.472(1)	0.485(1)	C(26b)	0.072(1)	-0.339(1)	0.510(1)
C(4a)	0.155(1)	0.412(1)	0.390(1)	C(27b)	0.006(1)	-0.323(1)	0.504(2)
C(5a)	0.177(1)	0.350(1)	0.3710(10)	C(28b)	-0.0467(8)	-0.2388(9)	0.4613(9)
C(6a)	0.2362(8)	0.3463(8)	0.4462(8)	C(29b)	0.1127(7)	-0.2882(7)	0.2454(8)
C(7a)	0.092(1)	0.416(1)	0.305(1)	C(30b)	0.1078(7)	-0.3677(7)	0.1787(7)
C(8a)	0.261(1)	0.2824(9)	0.4148(9)	C(31b)	0.0441(7)	-0.4557(7)	0.1586(8)
C(9a)	0.346(1)	0.2235(9)	0.4137(10)	C(32b)	0.0464(9)	-0.5257(8)	0.1049(9)
C(10a)	0.434(1)	0.287(1)	0.411(1)	C(33b)	0.110(1)	-0.5069(10)	0.0693(10)
C(11a)	0.564(1)	0.440(1)	0.500(1)	C(34b)	0.1746(9)	-0.4193(10)	0.0852(9)
C(12a)	0.559(1)	0.3237(10)	0.548(1)	C(35b)	0.1700(8)	-0.3507(7)	0.1389(8)
C(13a)	0.5971(9)	0.3613(9)	0.658(1)	C(1s)	0.622(1)	0.142(1)	0.920(1)
C(14a)	0.5130(8)	0.2926(7)	0.7420(9)	C(2s)	0.758(1)	0.245(1)	1.077(1)
C(15a)	0.3797(7)	0.2853(6)	0.7730(7)	C(3s)	0.649(1)	0.082(1)	1.037(1)
C(16a)	0.4418(7)	0.2601(6)	0.7768(7)				

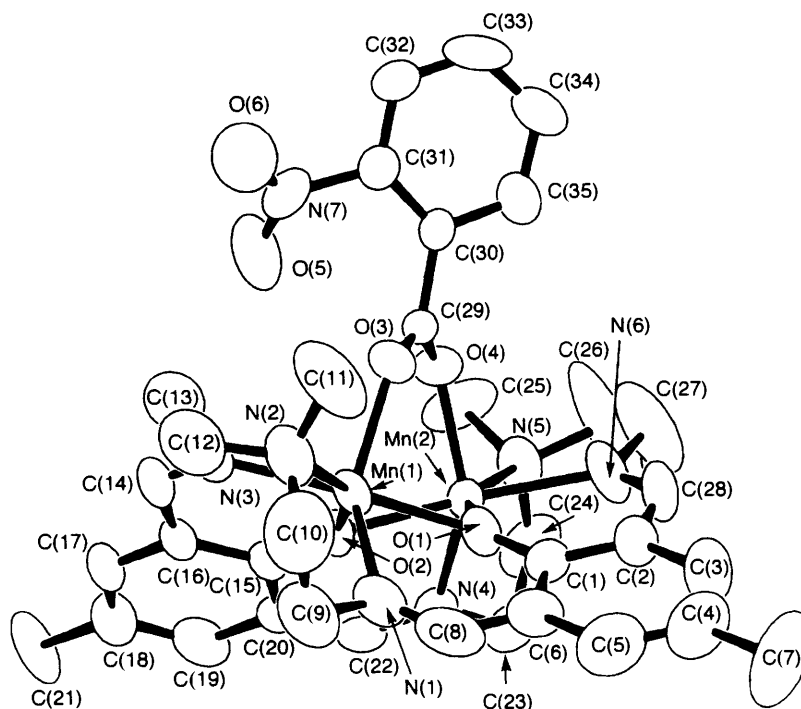
\* Suffixes a, b, s denote molecule (complex cation) A, molecule B, perchlorate anions and dimethylformamide solvent molecule, respectively.

force the two phenol rings to be more 'spread out' in this molecule, which results in the large angle between O(1a)-C(1a) and O(2a)-C(15a). In molecule B, the packing is less tight; one of the phenol rings has only two contacts with the molecule B' [C(4b) and C(6b)]; as for the other phenol ring, the shortest intermolecular distance is 3.87(1) Å between C(19b) and C(17a). The looser environment allows molecule B to have a smaller angle between O(1b)-C(1b) and O(2b)-C(15b), compared with molecule A. It is noteworthy that the corresponding angles are still larger than in the related complexes  $[\text{Mn}_2\text{L}(\text{MeCO}_2)]\text{ClO}_4$  and  $[\text{Mn}_2\text{LCl}]\text{ClO}_4$ <sup>11</sup> [106.8(4) and 101.7(5)°, respectively].

**FAB-MS Spectra and Exchange of the Bridging Anion.**—The FAB-MS spectrum (in 3-nitrobenzyl alcohol matrix) of the previously reported chloride complex  $[\text{Mn}_2\text{LCl}]\text{ClO}_4$ <sup>11</sup> showed two prominent peaks at *m/z* 633 and 764. The former was assigned to  $[\text{Mn}_2\text{LCl}]^+$ , and the latter corresponded to  $[\text{Mn}_2\text{L}(3\text{-O}_2\text{NC}_6\text{H}_4\text{CO}_2)]^+$ , which was formed by the action of 3-nitrobenzoic acid present in 3-nitrobenzyl alcohol as an impurity. Actually, this peak was absent when 3-nitrobenzyl alcohol was carefully purified prior to use. Moreover, deliberate addition of various substituted benzoic acids (RCO<sub>2</sub>H) to the matrix led to formation of the corresponding benzoate

**Table 2** Selected bond lengths (Å) and angles (°) for  $[\text{Mn}_2\text{L}(2\text{-O}_2\text{NC}_6\text{H}_4\text{CO}_2)]\text{ClO}_4 \cdot 0.5\text{Me}_2\text{NCHO}$ 

	Molecule A	Molecule B		Molecule A	Molecule B
Mn(1)–N(1)	2.184(10)	2.175(8)	Mn(2)–N(4)	2.171(8)	2.166(8)
Mn(1)–N(2)	2.55(1)	2.472(8)	Mn(2)–N(5)	2.435(9)	2.535(9)
Mn(1)–N(3)	2.208(9)	2.217(9)	Mn(2)–N(6)	2.230(9)	2.173(9)
Mn(1)–O(1)	2.197(7)	2.187(6)	Mn(2)–O(1)	2.134(7)	2.184(6)
Mn(1)–O(2)	2.148(6)	2.163(6)	Mn(2)–O(2)	2.193(6)	2.208(6)
Mn(1)–O(3)	2.115(7)	2.117(7)	Mn(2)–O(4)	2.105(7)	2.106(7)
N(1)–Mn(1)–N(2)	70.7(4)	73.3(3)	N(4)–Mn(2)–N(5)	71.2(3)	70.6(3)
N(1)–Mn(1)–N(3)	116.9(4)	103.3(3)	N(4)–Mn(2)–N(6)	113.9(3)	105.1(4)
N(2)–Mn(1)–N(3)	73.2(4)	74.8(3)	N(5)–Mn(2)–N(6)	72.9(3)	73.7(4)
O(1)–Mn(1)–N(1)	79.1(3)	81.1(3)	O(1)–Mn(2)–N(4)	116.1(3)	121.4(3)
O(1)–Mn(1)–N(2)	132.2(3)	128.2(3)	O(1)–Mn(2)–N(5)	153.3(3)	153.8(3)
O(1)–Mn(1)–N(3)	154.6(3)	156.2(3)	O(1)–Mn(2)–N(6)	81.0(3)	80.4(3)
O(1)–Mn(1)–O(2)	75.2(2)	76.3(2)	O(1)–Mn(2)–O(2)	75.5(2)	75.5(2)
O(1)–Mn(1)–O(3)	87.0(3)	94.4(3)	O(1)–Mn(2)–O(4)	95.4(3)	99.5(3)
O(2)–Mn(1)–N(1)	114.1(3)	121.2(3)	O(2)–Mn(2)–N(4)	79.1(3)	80.6(3)
O(2)–Mn(1)–N(2)	151.2(3)	155.0(3)	O(2)–Mn(2)–N(5)	130.6(3)	130.7(3)
O(2)–Mn(1)–N(3)	80.0(3)	81.6(3)	O(2)–Mn(2)–N(6)	156.5(3)	154.3(3)
O(2)–Mn(1)–O(3)	100.7(3)	94.6(3)	O(2)–Mn(2)–O(4)	89.3(3)	92.5(3)
O(3)–Mn(1)–N(1)	137.2(3)	141.1(3)	O(4)–Mn(2)–N(4)	141.8(3)	134.5(3)
O(3)–Mn(1)–N(2)	90.8(3)	79.9(3)	O(4)–Mn(2)–N(5)	90.6(3)	81.3(3)
O(3)–Mn(1)–N(3)	92.1(3)	96.1(3)	O(4)–Mn(2)–N(6)	90.7(3)	100.2(4)

**Fig. 1** A perspective view of  $[\text{Mn}_2\text{L}(2\text{-O}_2\text{NC}_6\text{H}_4\text{CO}_2)]^+$ . Only one of the two crystallographically independent complex cations (molecule A) is shown

complexes  $[\text{Mn}_2\text{L}(\text{RCO}_2)]^+$ . These results clearly show that exchange of the bridging anion takes place quite easily in this chloride-bridged complex.

The benzoate-bridged complexes  $[\text{Mn}_2\text{L}(\text{RCO}_2)]^+$ , also showed similar exchange reactions. The FAB-MS spectra of  $[\text{Mn}_2\text{L}(\text{RCO}_2)]^+$  in the presence of another benzoic acid  $\text{R}'\text{CO}_2\text{H}$  always indicated formation of the exchange product  $[\text{Mn}_2\text{L}(\text{R}'\text{CO}_2)]^+$ . The amount of the exchange product formed increased with increasing basicity of the benzoate anion.

Such exchange reactions are also useful from a synthetic

point of view. When an equimolar mixture of sodium benzoate and  $[\text{Mn}_2\text{LCl}]\text{PF}_6$  was heated to reflux in methanol,  $[\text{Mn}_2\text{L}(\text{PhCO}_2)]\text{PF}_6$  was obtained in 66% yield.

*Cyclic Voltammetry.*—The cyclic voltammograms of complexes  $[\text{MnL}(\text{RCO}_2)]\text{ClO}_4$  showed two reversible waves in the range 0.0–1.0 V (vs. ferrocene–ferrocenium couple, in acetonitrile–0.1 mol  $\text{dm}^{-3}$   $\text{NEt}_4\text{ClO}_4$ ). The two waves correspond to  $\text{Mn}^{\text{II}}\text{Mn}^{\text{II}}\text{–Mn}^{\text{II}}\text{Mn}^{\text{III}}$  and  $\text{Mn}^{\text{II}}\text{Mn}^{\text{III}}\text{–Mn}^{\text{III}}\text{Mn}^{\text{III}}$  couples. The half-wave potentials ( $E_{1/2}^1$  and  $E_{1/2}^2$ ) showed

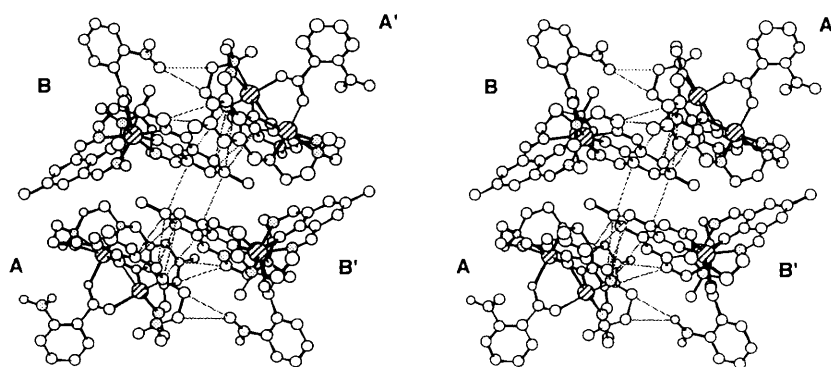


Fig. 2 Packing diagram of  $[\text{Mn}_2\text{L}(2\text{-O}_2\text{NC}_6\text{H}_4\text{CO}_2)]^+$ . The two independent complex cations are denoted A and B; A' and B' are the symmetry-related molecules ( $-x, -y, 1-z$ ). Broken lines indicate short contacts ( $< 3.60 \text{ \AA}$ ). Perchlorate anions and solvent molecules are omitted

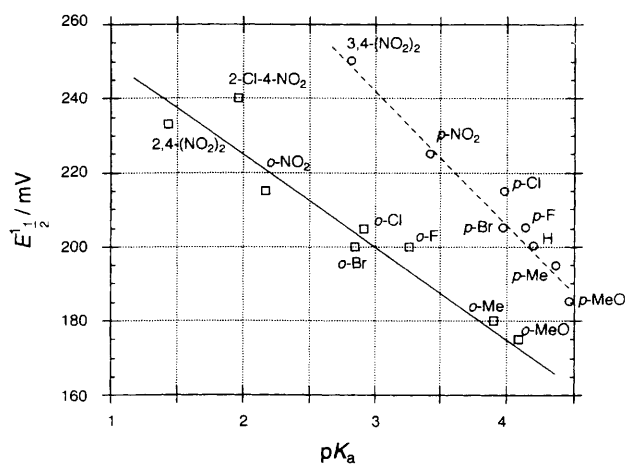


Fig. 3 A plot of first oxidation potential  $E_{1/2}^1$  of  $[\text{Mn}_2\text{L}(\text{RCO}_2)]\text{ClO}_4$  vs.  $\text{p}K_a$  of the conjugate acid ( $\text{RCO}_2\text{H}$ ) of the bridging benzoate

Table 3 Important intermolecular contacts ( $< 3.60 \text{ \AA}$ ) for  $[\text{Mn}_2\text{L}(2\text{-O}_2\text{NC}_6\text{H}_4\text{CO}_2)]\text{ClO}_4 \cdot 0.5\text{Me}_2\text{NCHO}^*$

N(4a) ... C(2b')	3.50(1)	C(22a) ... C(5b')	3.47(1)
N(4a) ... C(3b')	3.55(1)	C(22a) ... C(4b')	3.50(1)
C(3a) ... C(27b')	3.43(2)	C(23a) ... C(6b')	3.24(1)
C(4a) ... C(27b')	3.60(2)	C(24a) ... O(6b')	3.36(1)
C(15a) ... C(7b')	3.48(1)	C(4b) ... C(6b')	3.49(1)
C(20a) ... C(4b')	3.43(1)		

\* Primed atoms are related to unprimed equivalents by the symmetry operation  $-x, -y, -z + 1$ .

systematic changes for the various bridging benzoates, similar to the previously reported acetate based complexes  $[\text{Mn}_2\text{L}(\text{R}'\text{CO}_2)]\text{ClO}_4$ .<sup>11</sup> A plot of  $E_{1/2}^1$  vs.  $\text{p}K_a$  of the bridging benzoate is shown in Fig. 3, which shows two independent linear correlations for the *ortho*- and *para*-substituted series.

**Catalytic Activity for Disproportionation of Hydrogen Peroxide.**—Similarly to previously reported acetate/halide bridged complexes  $[\text{Mn}_2\text{L}(\text{R}'\text{CO}_2)]\text{ClO}_4$ ,<sup>11</sup> the benzoate complexes  $[\text{Mn}_2\text{L}(\text{RCO}_2)]\text{ClO}_4$  effectively catalysed disproportionation of hydrogen peroxide. When an  $\text{H}_2\text{O}_2$  solution ( $8.35 \text{ mol dm}^{-3}$ ) in MeCN ( $1 \text{ cm}^3$ ) was added to a solution of  $[\text{Mn}_2\text{L}(\text{RCO}_2)]\text{ClO}_4$  ( $5 \times 10^{-3} \text{ mol dm}^{-3}$ ) in MeCN ( $10 \text{ cm}^3$ ), gaseous dioxygen was evolved as shown in Fig. 4 and hydrogen peroxide was almost completely consumed. After completion of the reaction, the starting complex was recovered in 77% yield. These results show that the ' $\text{Mn}_2\text{L}(\text{RCO}_2)$ ' core serves as a very effective and robust device for evolution of dioxygen.

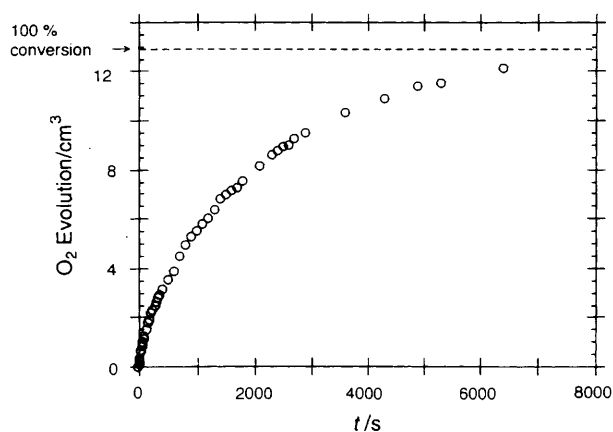


Fig. 4 Time profile of the evolution of oxygen by disproportionation of  $\text{H}_2\text{O}_2$  catalysed by  $[\text{Mn}_2\text{L}(\text{PhCO}_2)]\text{ClO}_4$

The initial maximum rate of  $\text{O}_2$  evolution (hereafter stated as  $V_{\text{max}}$ ; the number of released  $\text{O}_2$  molecules per molecule of complex per second) was determined for various benzoate complexes  $[\text{Mn}_2\text{L}(\text{RCO}_2)]\text{ClO}_4$ . Since it has been reported that addition of base causes acceleration of manganese-catalysed  $\text{O}_2$  evolution,<sup>5,6</sup> experiments in the presence of 2,4,6-trimethylpyridine were also performed. The results are shown in Fig. 5, together with those for substituted acetate complexes  $[\text{Mn}_2\text{L}(\text{R}'\text{CO}_2)]\text{ClO}_4$  ( $\text{R}' = \text{CH}_3, \text{CCl}_3, \text{CF}_3, \text{CHCl}_2$  or  $\text{CH}_2\text{Cl}$ ). The horizontal scale is the  $\text{p}K_a$  value (in water) of corresponding acid  $\text{RCO}_2\text{H}$  or  $\text{R}'\text{CO}_2\text{H}$ .

We previously reported<sup>11</sup> that the acetate based complexes  $[\text{Mn}_2\text{L}(\text{R}'\text{CO}_2)]\text{ClO}_4$  showed increasing activity with increasing acidity of the corresponding acid  $\text{R}'\text{CO}_2\text{H}$ , and proposed that dissociation of the bridging  $\text{R}'\text{CO}_2^-$  is involved in the rate-determining step (the more acidic the acid, the less basic is the conjugate base, and therefore more readily it dissociates). However, in the present study the situation is more complicated. In the presence of 2,4,6-trimethylpyridine, the activity increases with increasing acidity of  $\text{RCO}_2\text{H}$ , as found previously. On the other hand, in the absence of 2,4,6-trimethylpyridine the activity decreases with increasing acidity of  $\text{RCO}_2\text{H}$ , reaches a minimum at  $\text{p}K_a \approx 2$ , and then rises again for stronger acids ( $\text{p}K_a < 2$ ).

In order to interpret these results, we focus on the effect of protonation of the complex upon dissociation of the bridging carboxylate. The complex  $[\text{Mn}_2\text{L}(\text{RCO}_2)]^+$  acts as a Brønsted base, as shown by pH measurements (glass electrode) in aqueous acetonitrile (see Experimental section). It is likely that in those complexes with a more basic  $\text{RCO}_2^-$  group (*i.e.* larger  $\text{p}K_a$ ) which is reluctant to dissociate, protonation of the complex is necessary prior to dissociation of the carboxylate. In

such circumstances, the  $O_2$ -evolving reaction has two pathways (Scheme 1). In the region of  $pK_a < 2$ , pathway (i), in which the reaction rate increases for less basic carboxylate; on the contrary, in the region of  $pK_a > 2$ , the pathway (ii) becomes dominant, in which the rate decreases for less basic carboxylate. The effect of 2,4,6-trimethylpyridine is two-fold; (i) to suppress the lower path by consuming  $H^+$ , and (ii) to accelerate the overall reaction by generating  $HO_2^-$  from  $H_2O_2$ .

In summary, the catalytic activities of manganese complexes  $[Mn_2L(RCO_2)]ClO_4$  and  $[Mn_2L(R'CO_2)]ClO_4$ <sup>11</sup> heavily depend on the nature of the bridging carboxylate. The basicity of the carboxylate is one of the most important factors in determining the activity. This conclusion will be useful in designing efficient oxygen-evolving systems for artificial photosynthesis models in the future.

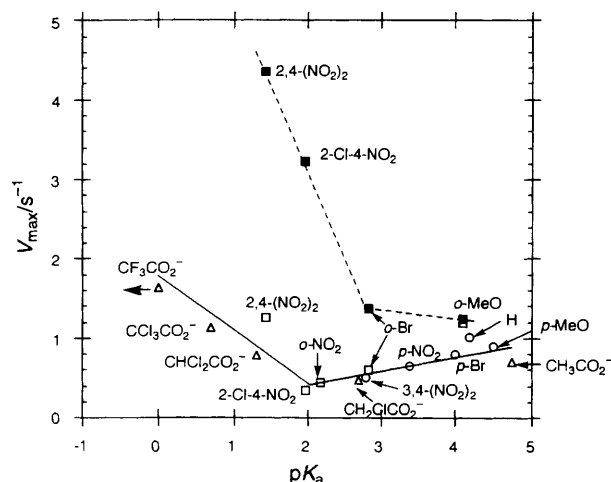
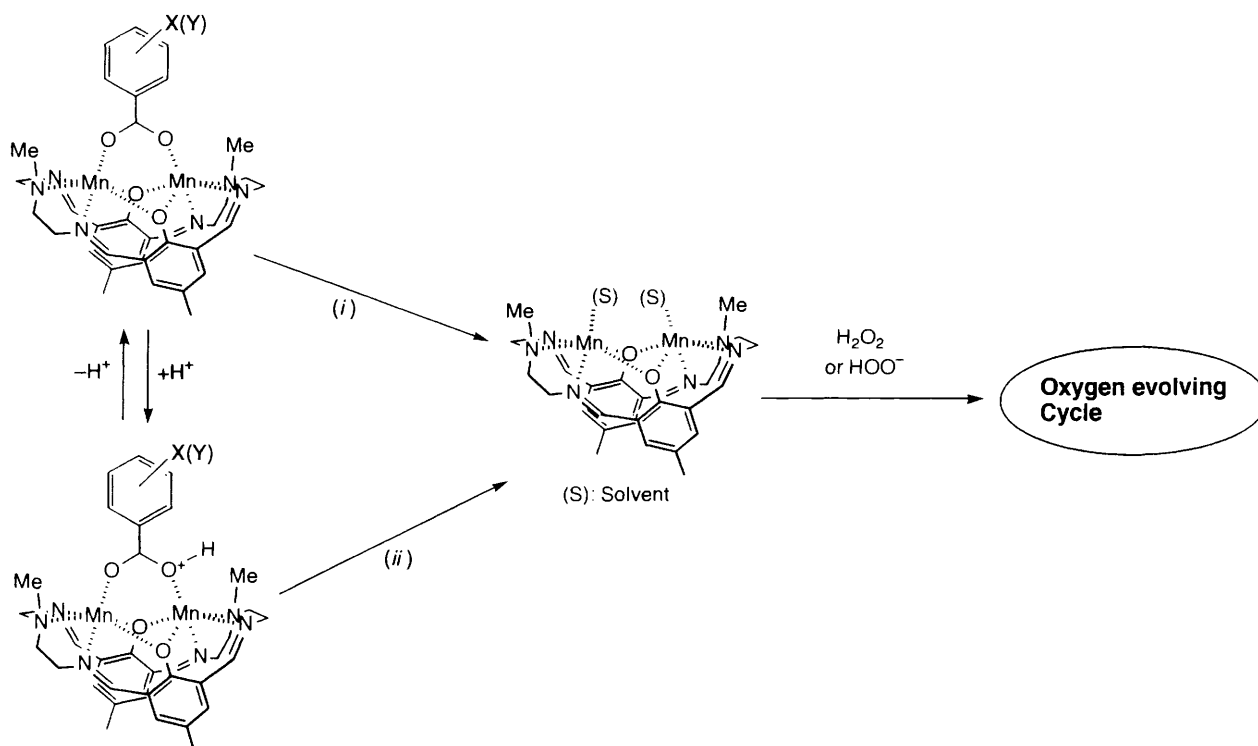


Fig. 5 A plot of initial rate of oxygen evolution ( $V_{max}$ ) vs.  $pK_a$  of the conjugate acid of the bridging carboxylate in absence (open symbols) or presence (filled symbols) of 2,4,6-trimethylpyridine



Scheme 1 Proposed mechanism of formation of active catalyst from  $[Mn_2L(RCO_2)]ClO_4$ . (i) Less basic  $RCO_2^-$ ,  $-RCO_2^-$ ; (ii) more basic  $RCO_2H$ ,  $-RCO_2H$

## Experimental

**General.**—Acetonitrile was distilled from  $CaH_2$ . Commercial hydrogen peroxide (90%) was distilled under reduced pressure and titrated (iodometry) before use. *N,N*-Bis(2-aminoethyl)-methylamine and other chemicals were purchased from Nacalai Tesque Co. or Tokyo Kasei Co. and used without further purification.

The FAB-MS spectra were obtained with an HX-110 mass spectrometer (JEOL), operating at 10 kV and Xe primary ion source; the matrix was 3-nitrobenzyl alcohol, which was purified when necessary by passing a column of activated alumina (Wako Pure Chemicals Co.) and distillation. Cyclic voltammetry measurements were performed with a Fuso 321B potentiostat and 312B function generator and 1.0 mm glassy carbon working electrode, in acetonitrile containing 0.1 mol  $dm^{-3}$   $NET_4ClO_4$ . Elemental analyses were performed at the Microanalysis Center of Kyoto University.

**Synthesis of  $[Mn_2L(RCO_2)]ClO_4$ .**—*N,N*-Bis(2-aminoethyl)-methylamine (180 mg, 1.52 mmol), 2,6-diformyl-4-methylphenol<sup>13</sup> (250 mg, 1.52 mmol),  $RCO_2H$  (1.52 mmol), NaOH (100 mg, 1.52 mmol) and  $Mn(ClO_4)_2 \cdot 6H_2O$  (550 mg, 1.52 mmol) were dissolved in methanol (20  $cm^3$ ) and the solution heated to reflux for 30 min. Sodium perchlorate (374 mg, 3.5 mmol) was added and the mixture heated for 15 min. Evaporation of half of the methanol yielded a yellow precipitate, which was collected by filtration. Yield 55–90%. **CAUTION:** Perchlorate salts of organic complexes are potentially explosive and should be handled with extreme care.

**Crystallographic Study of  $[Mn_2L(2-O_2NC_6H_4CO_2)]ClO_4 \cdot 0.5Me_2NCHO$ .**—Single crystals of  $[Mn_2L(2-O_2NC_6H_4CO_2)]ClO_4 \cdot 0.5Me_2NCHO$  were grown by vapour diffusion of  $Et_2O$  into a dimethylformamide solution of the complex. A yellow crystal with dimensions 0.50 × 0.20 × 0.20 mm was mounted on a glass fibre and coated with an epoxy resin. Data collection was made at room temperature on a Rigaku AFC7R diffractometer with Cu- $K\alpha$  radiation ( $\lambda = 1.54178 \text{ \AA}$ ) from a 12 kW rotating anode generator, using the  $\omega$ -2 $\theta$

scanning technique to a maximum  $2\theta$  value of  $120.1^\circ$ . Cell constants and an orientation matrix were obtained from a least-squares refinement of 25 reflections ( $55 < 2\theta < 66^\circ$ ). Three standard reflections measured after every 150 revealed 7.0% decay during the course of data collection; the data were corrected by a linear correction factor based on the standard intensities. Empirical absorption correction was applied based on  $\psi$ -scans of three reflections ( $\chi = 78\text{--}102^\circ$ ); the transmission coefficients ranged from 0.62 to 1.00. Of 12 569 reflections collected 12 021 were unique ( $R_{\text{int}} = 0.067$ ), 6297 observed [ $I > 3\sigma(I)$ ]. The structure was solved by direct methods (SIR 88).<sup>14</sup> All non-hydrogen atoms were refined anisotropically, while hydrogen atoms of methylene, methine and phenyl groups were fixed at the calculated positions. The final cycle of full-matrix least-squares refinement (1036 variable parameters) gave  $R = 0.066$ ,  $R' = 0.069$  ( $R = \Sigma(|F_o| - |F_c|)/\Sigma|F_o|$ ,  $R' = \Sigma w(|F_o| - |F_c|)^2/\Sigma w(|F_o|)^2$  where  $w^{-1} = \sigma^2(F_o)$ ). The maximum and minimum peaks on the final difference Fourier map were 0.63 and  $-0.53 \text{ e } \text{Å}^{-3}$ . All the calculations were performed using the TEXSAN<sup>15</sup> software package of Molecular Structure Corporation.

Crystal data for  $[\text{Mn}_2\text{L}(2\text{-O}_2\text{NC}_6\text{H}_4\text{CO}_2)]\text{ClO}_4 \cdot 0.5\text{Me}_2\text{NCHO}$ :  $\text{C}_{36.5}\text{H}_{43.5}\text{ClMn}_2\text{N}_{7.5}\text{O}_{10.5}$ ,  $M = 900.62$ , triclinic, space group  $P\bar{1}$ ,  $a = 18.117(6)$ ,  $b = 18.781(6)$ ,  $c = 15.452(3) \text{ Å}$ ,  $\alpha = 104.71(2)$ ,  $\beta = 104.03(2)$ ,  $\gamma = 118.56(2)^\circ$ ,  $U = 4036(2) \text{ Å}^3$ ,  $D_c = 1.482 \text{ g cm}^{-3}$  for  $Z = 4$ ,  $F(000) = 1864$ .

Additional material available from the Cambridge Crystallographic Data Centre comprises H-atom coordinates, thermal parameters and remaining bond lengths and angles.

**Solution pH Measurements in the Absence and Presence of Manganese Complex.**—pH Measurements in aqueous acetonitrile were performed with a Horiba F-22 pH meter, a glass electrode (for non-aqueous solvents) and Ag–AgClO<sub>4</sub> (10 mmol dm<sup>-3</sup> in MeCN) reference electrode. Acetonitrile–water ( $v/v = 10:1$ ) containing 0.04 mol dm<sup>-3</sup> NEt<sub>4</sub>ClO<sub>4</sub> was used. All measurements were carried out at 25 °C. The electrode was calibrated with HClO<sub>4</sub> solutions of known concentration. The potentials (relative to the Ag–AgClO<sub>4</sub> reference) for concentrations of  $9 \times 10^{-3}$ ,  $2.7 \times 10^{-3}$ ,  $9 \times 10^{-4}$ ,  $8.1 \times 10^{-5}$ ,  $9 \times 10^{-5}$  and  $2.4 \times 10^{-6} \text{ mol dm}^{-3}$  were 56, 25,  $-10$ ,  $-69$ ,  $-73$  and  $-243 \text{ mV}$ , respectively. A solution containing  $2.4 \times 10^{-4} \text{ mol dm}^{-3}$   $[\text{Mn}_2\text{L}(\text{RCO}_2)]\text{ClO}_4$  and  $2.4 \times 10^{-4} \text{ mol dm}^{-3}$  HClO<sub>4</sub> showed potentials of  $-248$  to  $-252 \text{ mV}$ , indicating  $>99\%$  uptake of H<sup>+</sup> by the complex. The exact  $pK_b$  values of the complexes were not determined because of the slow and uncertain response of the glass electrode at  $[\text{H}^+] < 10^{-6} \text{ mol dm}^{-3}$ .

#### Acknowledgements

The authors thank Professor Atsuyoshi Ohno (Institute for Chemical Research, Kyoto University) for his kind permission

to use the X-ray diffractometer, Professor Atsuhiko Osuka (Kyoto University) for his kind permission to use the HX-110 mass spectrometer and the electrochemical apparatus, and Mr. Satoshi Nomura (Horiba Co.) for pH measurements.

#### References

- 1 Y. Kono and I. Fridovich, *J. Biol. Chem.*, 1983, **258**, 6015; G. S. Algood and J. J. Perry, *J. Bacteriol.*, 1986, **168**, 563; V. V. Barynin and A. I. Grebenko, *Dokl. Akad. Nauk, SSSR*, 1986, **286**, 461.
- 2 W. Vermaas, *Annu. Rev. Plant Physiol. Plant Mol. Biol.*, 1993, **44**, 457; R. J. Debus, *Biochim. Biophys. Acta*, 1992, **1102**, 269; O. Hansson and T. Wydrzynski, *Photosynth. Res.*, 1990, **23**, 131; K. Sauer, V. K. Yachandra, R. D. Britt and M. P. Klein, in *Manganese Redox Enzymes*, ed. V. L. Pecoraro, VCH, New York, 1992, p. 141.
- 3 P. J. Pessiki, S. V. Khangulov, D. M. Ho and G. C. Dismukes, *J. Am. Chem. Soc.*, 1994, **116**, 891; P. J. Pessiki and G. C. Dismukes, *J. Am. Chem. Soc.*, 1994, **116**, 898.
- 4 E. J. Larson and V. L. Pecoraro, *J. Am. Chem. Soc.*, 1991, **113**, 3810, 7809.
- 5 Y. Naruta and K. Maruyama, *J. Am. Chem. Soc.*, 1991, **113**, 3595; Y. Naruta, M. Sasayama and T. Sasaki, *Angew. Chem., Int. Ed. Engl.*, 1994, **33**, 1839; Y. Naruta and M. Sasayama, *J. Chem. Soc., Chem. Commun.*, 1994, 2667; *Chem. Lett.*, 1994, 2411.
- 6 P. Battioni, J. P. Renaud, J. F. Bartoli, M. Reina-Artiles, M. Fort and D. Mansuy, *J. Am. Chem. Soc.*, 1988, **110**, 8462.
- 7 U. Bossek, M. Saher, T. Weyhermueller and K. Wieghardt, *J. Chem. Soc., Chem. Commun.*, 1992, 1780.
- 8 S. Wang, H.-L. Tsai, K. S. Hagen, D. N. Hendrickson and G. Christou, *J. Am. Chem. Soc.*, 1994, **116**, 8376.
- 9 M. Watkinson, A. Whiting and C. A. McAuliffe, *J. Chem. Soc., Chem. Commun.*, 1994, 2141; N. Aurangzeb, C. E. Hulme, C. A. McAuliffe, R. G. Pritchard, M. Watkinson, M. R. Bermejo, A. Garcia-Deibe, M. Rey, J. Sanmartin and A. Sousa, *J. Chem. Soc., Chem. Commun.*, 1994, 1153.
- 10 C. Higuchi, H. Sakiyama, H. Okawa, R. Isobe and D. E. Fenton, *J. Chem. Soc., Dalton Trans.*, 1994, 1097; H. Sakiyama, H. Okawa and R. Isobe, *J. Chem. Soc., Chem. Commun.*, 1993, 882.
- 11 Y. Ikawa, T. Nagata and K. Maruyama, *Chem. Lett.*, 1993, 1049; T. Nagata, Y. Ikawa and K. Maruyama, *J. Chem. Soc., Chem. Commun.*, 1994, 471.
- 12 H.-R. Chang, S. K. Larsen, P. D. W. Boyd, C. G. Pierpont and D. N. Hendrickson, *J. Am. Chem. Soc.*, 1988, **110**, 4565; A. J. Downard, V. McKee and S. S. Tandon, *Inorg. Chim. Acta*, 1990, **173**, 181; A. J. Edwards, B. F. Hoskins, R. Robson, J. C. Wilson, B. Moubaraki and K. S. Murray, *J. Chem. Soc., Dalton Trans.*, 1994, 1837.
- 13 F. Ullmann and K. Brittner, *Chem. Ber.*, 1909, **42**, 2539.
- 14 M. C. Burla, M. Camalli, G. Cascarano, C. Giacovazzo, G. Polidori, R. Spagna and D. Viterbo, *J. Appl. Crystallogr.*, 1989, **22**, 389.
- 15 TEXSAN, Crystal Structure Analysis Package, Molecular Structure Corporation, The Woodlands, TX, 1985, 1992.

Received 3rd January 1995; Paper 5/00004A